Hypsometry of Martian Terrains from Earth-based Radar Measurements

P. J. Mouginis-Mark, Department of Geological Sciences, Brown University, Providence, RI 02912; and S. H. Zisk, NEROC Haystack Observatory, Westford MA 01886.

Introduction: The Goldstone radar measurements of Mars made during the 1971 and 1973 oppositions (1) generated a wealth of data that has enabled the topography and surface characteristics of the planet to be investigated (e.g., refs. 2-4). Together with parameters not considered here, these radar measurements provided information on martian topography with an areal resolution of 80 km in latitude and 10 km in longitude, with a height accuracy of about 100 meters (1). The data cover almost the entire circumference of the planet for the latitude band 14-22°S and contain approximately 32,000 point estimates of elevation above the reference ellipsoid of Standish (5). As such, these measurements represent an extensive data set with which to investigate the hypsometric properties of Mars.

Previous investigations of martian hypsometry (6,7) have concentrated on a global analysis using the variety of data employed to generate the U. S. Geological Survey topographic map of Mars (8). Radar-derived contour maps have also been generated for specific regions of Mars to support other investigations (2, 4). As with the other attributes of the radar data (the estimates of surface roughness and inherent reflectivity) (4), however, the Goldstone altimetry measurements also permit specific terrain types on Mars to be characterized solely on the basis of their radar properties. This can be achieved by the analysis of the distribution of radar height measurements for knowngeological regions of the planet.

Data Analysis: As examples of this technique, we present in Fig. 1 radar-derived hypsometric histograms for five well defined surface materials on Mars. Each histogram in Fig. 1 presents all the point estimates of surface topography within a 5° x 5° latitude/longitude sample bin. Between 248 and 440 data points were used for each of these 12 samples. The areas investigated in Fig. 1 were specifically chosen because they represent distinctive surface materials on Mars. Based on the geological mapping of Scott and Carr (9), and subsequent refinements from Viking images (e.g., refs. 10, 11), these areas correspond to: 1) Tharsis lavas south of Arsia Mons; 2) Ridged plains materials within Sinai Planum; 3) Canyon lands around Eos Chasma; 4) Cratered plateau materials in Sinus Sabaeus; and 5) Hilly and cratered materials in western Memnonia.

While obvious differences in the shapes of the hypsometric histograms shown in Fig. 1 are apparent, their direct relationships to the regional morphology of Mars can be more readily appreciated from a concurrent investigation of the prominent surface features within each area. Fig. 2 displays the positions of all craters larger than 5 km diameter that either possess ejecta blankets (solid outlines) or lack ejecta blankets (open outlines), together with the position of Eos Chasma for the canyons region. Illustrated in Fig. 2 is a strong trend for a greater number of larger impact craters to be associated with the change from Tharsis lavas, to ridged plains, cratered plateau, and hilly and cratered materials. A comparison between Figs. 1 and 2 illustrated that this trend is directly associated with the broadening of the hypsometric histograms, and the tendency for bi-modal and tri-modal elevation distributions to occur.

Interpretations: The hypsometric histograms of Fig. 1 are interpreted here to reflect gently sloping surfaces that have numerous depressed (crater floors) and raised (crater rims and wrinkle ridges) areas. Very sharp, nar-

row histograms are seen for the almost crater-free lavas south of Arsia Mons, while the low crater density of the ridged plains between 70-75°W causes only a slight (400 meter) broadening of the histogram. Suprisingly, the cratered plateau materials between 350-355°W appear relativley flat (800 meters of relief) despite several large craters greater than 50 km in diameter. The degraded nature of these craters, with their lack of prominent rims and ejecta blankets, is believed to be responsible for this situation. The histogram for 170-175°W is believed to be an excellent example of the tri-modal height distribution associated with heavily cratered terrains, while the regions between 65-70°, 175-180°, 345-350° and 355-360°W show only a bi-modal height distribution. These bi-modal histograms are believed to be the products of the terrain dichotomy between the crater floors and the surrounding plains units.

Roth et al. (ref. 2, their Fig. 21) noted that their probability density function for elevations (essentially similar to the technique employed in our Fig. 1) for the canyons between 14.16-16.69°S and 35-55°W showed a wide variation in altitude, equivalent to over 7 km of relief between the canyon rim and floor. This distribution is qualitatively supported in Fig. 1, which shows a strong peak in the number of measurements at the highest elevations (corresponding to the canyon rim), and the numerous randomly scattered low estimates (equivalent to the canyon floor and walls).

Conclusions: We conclude that the derivation of regional martian hypsometric histograms from the Goldstone radar data offers an alternative method for interpreting the size and number of impact craters on a given surface, together with the capability to recognize large-scale tectonic features such as canyons. In the case of Mars, this technique will probably be of value only when used in conjunction with additional analyses of the radar measurements (e.g., refs. 4, 12) or other data sets such as Viking Orbiter color images (13, 14) and thermal data (15, 16). In the cases of Pioneer Venus altimetry or Earth-based radar measurements of the surface of Mercury, however, we believe that radar-hypsometry offers intriguing possibilities for estimating such surface attributes as crater size/frequency distributions, the degree if crater erosion (particularly the preservation of rim topography) and regional tectonic features for planetary surfaces as yet unimaged by spacecraft.

References: 1) Downs G. S. et al. (1975) Icarus 26, 273-312. 2) Roth L. E. et al. (1980) Icarus 42, 287-316. 3) Schaber G. G. (1980) Icarus 42, 159-184. 4) Mouginis-Mark P. J. et al. (1980) PLPSC 11th, in press. 5) Standish E. M. (1973) Astron. Astrophys. 26, 463-466. 6) Mutch T. M. et al. (1976) The Geology of Mars, Princeton University Press, N.J., 400 p. 7) Coradini M. et al. (1980) The Moon and Planets 22, 201-210. 8) U. S. Geological Survey Map I-961. 9) Scott D. H. and Carr M. H. (1978) U. S. Geological Survey map I-1083. 10) Greeley R. and Spudis P. D. (1978) Geophys. Res. Lttrs. 5, 453-456. 11) Scott D. H. (1980) NASA-TM 81776, 372. 12) Zisk S. H. and Mouginis-Mark P. J. (1981) this vol. 13) Soderblom L. A. et al. (1978) Icarus 34, 446-464. 14) McCord T. B. et al. (1980) LPS XI, 697-699. 15) Kieffer H. H. et al. (1977) J. Geophys. Res. 82, 4249-4291. 16) Zimbelman J. R. and Kieffer H. H. (1979) J. Geophys. Res. 84, 8239-8251.

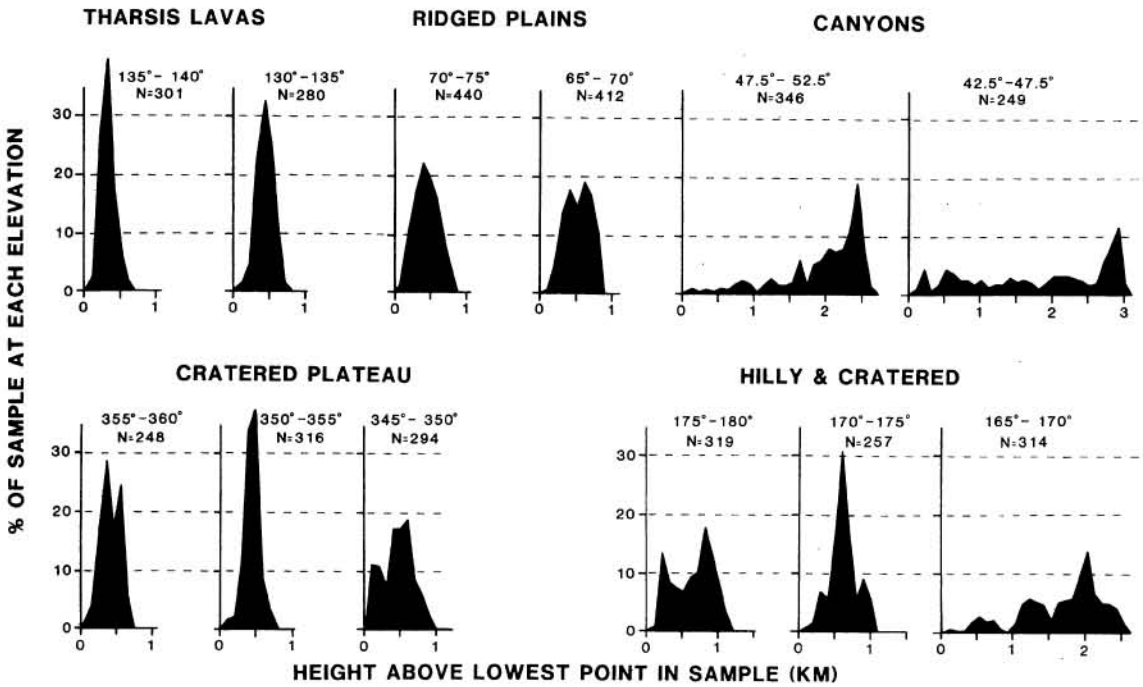

Figure 1: Radar-derived hypsometric histograms for five surface materials located between 15-20°S. Height measurements are taken from the análysis of Downs et al.(1), here referenced to an arbitrary datum set to the lowest elevation for each sample. "N" gives the size of each data sample. Bin size for height values is 200 meters.

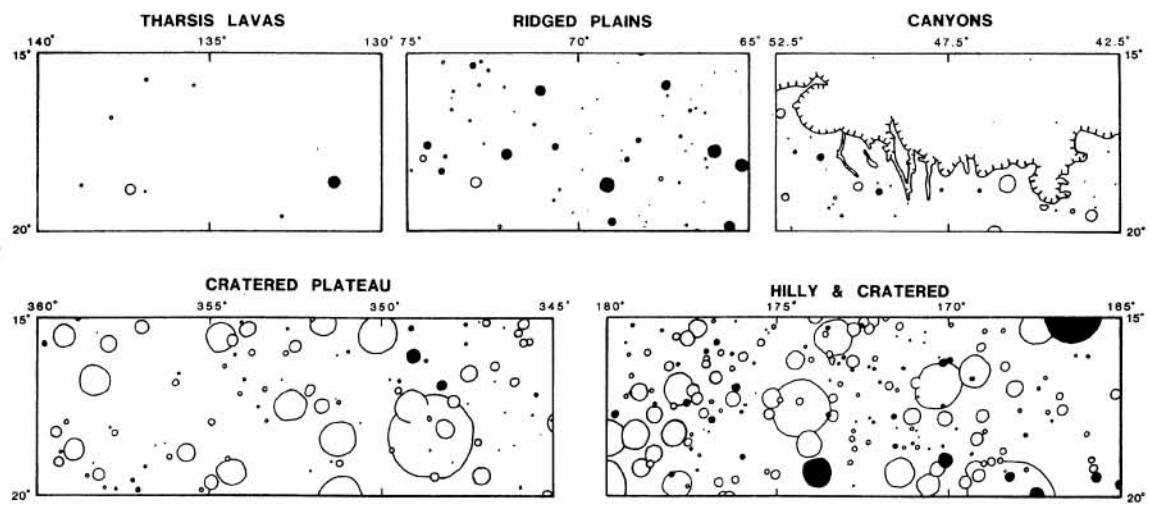

Figure 2: Distribution of all craters larger than 5 km diamters in the areas investigated here. Craters with solid outlines possess ejecta blankets, those craters without ejecta deposits are denoted by open outlines. Eos Chasma lies in the northern half of the Canyons sample.